Research Square

Preprints are preliminary reports that have not undergone peer review.
They should not be considered conclusive, used to inform clinical practice,
or referenced by the media as validated information.

Development and immunogenicity evaluation of a ferritin-based nanoparticle vaccine displaying porcine epidemic diarrhea virus spike receptor-binding domain in mice

Mo Zhou
Jiangsu Agri-animal Husbandry Vocational College
Nannan Nie
Nanjing Agricultural University
Li Zhang
Jiangsu Agri-animal Husbandry Vocational College
Changchun Chen
Jiangsu Agri-animal Husbandry Vocational College
Shinuo Cao
shinuo_cao@163.com
Jiangsu Agri-animal Husbandry Vocational College
Shanyuan Zhu
Jiangsu Agri-animal Husbandry Vocational College

Research Article

Keywords: PEDV, Ferritin, Spike protein receptor-binding domain, Subunit vaccine, Nanoparticle, Immunogenicity

Posted Date: September 7th, 2026

DOI: https://doi.org/10.21203/rs.3.rs-10663930/v1

License: This work is licensed under a Creative Commons Attribution 4.0 International License.
Read Full License

Additional Declarations: No competing interests reported.

Abstract

Background

Porcine epidemic diarrhea virus (PEDV) continues to pose a significant threat to the global swine industry, underscoring the urgent need for safe and effective vaccines. The spike (S) glycoprotein receptor-binding domain (RBD) is a promising subunit vaccine antigen; however, recombinant soluble S-RBD often exhibits limited immunogenicity due to structural instability and suboptimal antigen presentation. Ferritin-based nanoparticles can self-assemble into highly ordered nanostructures and present antigens in a multivalent manner, thereby enhancing immunogenicity and immune recognition. This study aimed to develop and evaluate a ferritin-based nanoparticle vaccine displaying PEDV S-RBD.

Results

A recombinant PEDV-S-RBD-FR fusion protein was designed, expressed in mammalian cells, purified, and successfully self-assembled into uniform nanoparticles with an average diameter of 27.37 nm, as confirmed by transmission electron microscopy. Immunization of mice with PEDV-S-RBD-FR elicited robust antigen-specific IgG responses, with endpoint antibody titers reaching 1:40,960 following booster immunization. Serum virus-neutralizing antibody titers of 1:64 were observed at day 42 post-immunization, and immune sera effectively inhibited PEDV infection in vitro. Additionally, elevated serum levels of IFN-γ and IL-4 indicated activation of both cellular and humoral immune responses, with a progressively enhanced Th1-biased immune profile characterized by an IFN-γ/IL-4 ratio above 1 at day 42.

Conclusions

These findings demonstrate that the ferritin-based PEDV-S-RBD nanoparticle vaccine efficiently induces strong humoral and cellular immune responses and generates functional neutralizing antibodies in mice. This self-assembling ferritin nanoparticle platform provides an effective strategy for enhancing antigen presentation and immunogenicity, supporting its potential as a promising vaccine candidate against PEDV.

Background

Porcine epidemic diarrhea virus (PEDV), an enveloped, positive-sense single-stranded RNA virus belonging to the genus Alphacoronavirus, is the etiological agent of porcine epidemic diarrhea (PED), one of the most devastating enteric diseases affecting the global swine industry. Since the emergence of highly virulent variant strains, particularly the GII genotype, PEDV outbreaks have caused substantial economic losses worldwide owing to high morbidity in pigs of all ages and exceptionally high mortality in neonatal piglets. PEDV primarily infects and replicates within intestinal epithelial cells, resulting in

severe villous atrophy, impaired nutrient absorption, and disruption of intestinal barrier function [1–4]. Clinically, infected pigs develop acute watery diarrhea, vomiting, dehydration, and rapid weight loss. Although adult pigs generally recover after transient disease, neonatal piglets frequently succumb to infection because of their immature immune system and limited intestinal regenerative capacity [3]. Moreover, the highly contagious fecal-oral transmission route, together with the continuous emergence of antigenically divergent strains, poses significant challenges for disease control [5, 6]. These characteristics highlight the limitations of current preventive measures and underscore the urgent need to develop more effective vaccines capable of eliciting broad and durable protective immunity.

The spike (S) glycoprotein of PEDV is the major surface protein responsible for viral attachment, receptor recognition, membrane fusion, and host cell entry, making it the principal target of protective immune responses [7–9]. Structurally, the S protein consists of two functional subunits, S1 and S2. The receptor-binding domain (RBD), located within the S1 subunit, mediates virus–host interactions and contains multiple conformational neutralizing epitopes that are essential for the induction of virus-neutralizing antibodies [10, 11]. Numerous studies have demonstrated that antibodies directed against the S-RBD effectively block viral attachment and entry, thereby preventing infection [12, 13]. Consequently, the S-RBD has been widely recognized as one of the most promising antigens for PEDV subunit vaccine development. Nevertheless, recombinant S protein or soluble S-RBD antigens often exhibit limited immunogenicity because of structural instability, suboptimal antigen presentation, and insufficient stimulation of B-cell activation, resulting in relatively weak neutralizing antibody responses [12]. Therefore, strategies that improve the structural presentation and immunogenicity of the S-RBD are expected to enhance the protective efficacy of PEDV subunit vaccines.

Nanoparticle-based antigen display has emerged as an effective approach for improving vaccine immunogenicity by mimicking the repetitive and highly ordered architecture of viral particles. Among the available nanoparticle platforms, ferritin has attracted considerable attention because of its ability to self-assemble into a stable 24-subunit nanocage with uniform size and geometry [14]. Fusion of antigens to ferritin enables their multivalent surface display, thereby increasing antigen density, promoting efficient cross-linking of B-cell receptors, facilitating antigen uptake by antigen-presenting cells, and ultimately enhancing both humoral and cellular immune responses [15]. Ferritin-based nanoparticle vaccines have shown encouraging immunogenicity against a variety of viral pathogens, including SARS-CoV-2, influenza virus, and porcine reproductive and respiratory syndrome virus (PRRSV) [16–18]. However, despite the biological importance of the PEDV S-RBD, the application of ferritin nanoparticles for multivalent presentation of this critical neutralizing antigen remains largely unexplored. Given that PEDV primarily infects the intestinal epithelium and that neutralizing antibodies against the S-RBD are critical for preventing viral entry, ferritin-mediated multivalent display of the S-RBD represents a rational strategy for improving vaccine-induced protective immunity [19].

In the present study, we developed a ferritin-based nanoparticle subunit vaccine displaying the PEDV S-RBD (PEDV-S-RBD-FR) through genetic fusion of the S-RBD to a self-assembling ferritin scaffold. The immunogenicity of the nanoparticle vaccine was systematically evaluated in a mouse model by

assessing antigen-specific antibody responses, cytokine production, and serum neutralizing activity. This study provides experimental evidence supporting the use of ferritin-mediated antigen display for PEDV vaccine development and offers a promising strategy for the rational design of next-generation nanoparticle-based subunit vaccines against PEDV.

Materials and Methods

Ethics statement

Animal experiments followed the national Regulations on the Administration of Experimental Animals from China's Ministry of Science and Technology. The experimental protocol obtained ethical clearance from the Scientific Ethics Committee of Jiangsu Agri-animal Husbandry Vocational College (Permit No. JSAHVC-2025-108).

Cells, plasmids, and reagents

Human embryonic kidney 293T (HEK293T) cells were routinely maintained in Dulbecco's modified Eagle's medium (DMEM) supplemented with 10% fetal bovine serum (FBS) and 1% penicillin–streptomycin (100 U/mL penicillin and 100 μg/mL streptomycin) at 37°C in a humidified atmosphere containing 5% CO_2. Chinese hamster ovary (CHO) cells were obtained commercially and maintained in CHO Grow® CD transient transfection serum-free medium at 37°C under 8% CO_2. The expression vector pCAGGS, the lentiviral vector pLVX-IRES-ZsGreen1, and the packaging plasmids psPAX2 and pMD2.G were available in our laboratory.

Construction of eukaryotic expression plasmids

The receptor-binding domain (RBD) of the PEDV spike (S) protein was fused to the N-terminus of ferritin via a flexible linker. A Kozak sequence (GCCACCATGG), a GT6 signal peptide (MGWSCIILFLVATATGVHS), and a 10×His tag were introduced upstream of the S-RBD sequence. EcoR I and Hind III restriction sites were incorporated at the 5' and 3' ends, respectively. The resulting genes were cloned into the pCAGGS vector to generate pCAGGS-PEDV-S-RBD-FR and pCAGGS-FR. Recombinant plasmids were verified by restriction enzyme digestion and Sanger sequencing (Fig. 1A).

Expression and characterization of recombinant proteins

HEK293T cells at 80–90% confluence were transfected with 2 μg plasmid using PolyJet™ reagent. After 6 h, the medium was replaced with DMEM containing 2% FBS, and cells were cultured for a further 48 h. Cells were lysed in RIPA buffer, and lysates were separated into soluble and insoluble fractions by centrifugation. Insoluble proteins were solubilized in 8 M urea. Protein samples were analyzed by SDS–

PAGE and Western blotting using an HRP-conjugated mouse anti-His antibody (1:3,000). Signals were detected by enhanced chemiluminescence (ECL).

Production of recombinant lentiviruses

Recombinant lentiviral vectors were generated by cloning the target gene into the *Eco*R I and *Bam*H I sites and verified by Sanger sequencing.

HEK293T cells were co-transfected with the transfer plasmid, psPAX2, and pMD2.G at a ratio of 3:2:1 using PolyJet™ reagent. After 6 h, the medium was replaced, and cells were cultured for 48 h. Viral supernatants were collected, clarified by centrifugation (6,000 rpm, 15 min, 4°C), filtered (0.45 μm), and concentrated by ultracentrifugation for downstream titration.

Expression and purification of ferritin nanoparticles

ExpiCHO cells (viability > 95%) were transduced with recombinant lentivirus (MOI = 20) in the presence of 8 μg/mL polybrene. GFP fluorescence was examined 48 h later to evaluate transduction efficiency. Cells were lysed in 8 M urea buffer, and His-tagged proteins were purified using immobilized metal affinity chromatography (IMAC)using magnetic beads. After washing with low-imidazole buffer, proteins were eluted with high-imidazole buffer and analyzed by SDS–PAGE and Western blotting.

Characterization of ferritin nanoparticles

Purified nanoparticles were refolded by dialysis against a buffer containing 50 mM Tris–HCl, 150 mM NaCl, 400 mM L-arginine, and 5% glycerol. Protein identity was confirmed by Western blotting. For TEM analysis, carbon-coated copper grids were glow-discharged (15 mA, 60 s), incubated with 4 μL of sample for 2 min, negatively stained with 3% uranyl acetate, air-dried, and imaged by transmission electron microscopy.

Mouse immunization and sample collection

Six-week-old female ICR mice were randomly divided into three groups (n = 5 per group): PEDV-S-RBD-FR, FR, and PBS. Mice were immunized intraperitoneally with 10 μg of antigen formulated with MF59 adjuvant on days 0, 14, and 28, whereas control mice received PBS with the same adjuvant. Blood samples were collected from the tail vein on days 0, 14, 28, and 42, and sera were separated and stored at − 80°C until use.

Indirect immunofluorescence assay (IFA)

HEK293T cells cultured in 96-well plates were transfected with pCAGGS-PEDV-S-RBD-FR or pCAGGS-FR (0.2 μg/well). At 48 h post-transfection, cells were fixed with 4% paraformaldehyde, permeabilized with

0.3% Triton X-100, and blocked. Serial two-fold dilutions of mouse sera collected on days 0, 14, 28, and 42 post-immunization were incubated with the cells for 2 h, followed by incubation with a fluorescent goat anti-mouse IgG secondary antibody for 1 h. Fluorescence was examined by a fluorescence microscopy, and endpoint antibody titers were determined as the highest serum dilution exhibiting specific fluorescence.

Measurement of serum cytokines by ELISA

Serum IFN-γ and IL-4 concentrations were measured using commercial ELISA kits (Shanghai Enzyme-linked Biotechnology Co., Ltd., China) according to the manufacturer's instructions. Absorbance was recorded at 450 nm using a microplate reader, and cytokine concentrations were calculated from standard curves generated using serially diluted standards.

Virus neutralization test

Serum samples collected on day 42 post-immunization were serially two-fold diluted (1:4 – 1:512), mixed with an equal volume of PEDV (200 $TCID_{50}$/100 μL), and incubated at 37°C for 1 h before inoculation onto Vero cell monolayers. After 5 days, viral infection was detected by IFA using a mouse anti-PEDV primary antibody and a fluorophore-conjugated goat anti-mouse IgG secondary antibody. The neutralizing antibody titer was defined as the highest serum dilution that completely prevented detectable fluorescence.

Statistical analysis

Statistical analyses were performed using GraphPad Prism 8.0 (GraphPad Software, La Jolla, CA, USA). Differences between two groups were analyzed using an unpaired Student's t-test, whereas comparisons among multiple groups were performed by one-way analysis of variance (ANOVA). Data are presented as the mean ± standard error of the mean (SEM). A P value < 0.05 was considered statistically significant.

Results

Construction and characterization of PEDV-S-RBD-FR expression constructs

The recombinant eukaryotic expression plasmids pCAGGS-PEDV-S-RBD-FR and pCAGGS-FR were confirmed by Sanger sequencing and double digestion with EcoR I and Hind III. Restriction analysis yielded the expected fragment sizes, including the pCAGGS backbone (4244 bp) and the insert fragments corresponding to PEDV-S-RBD-FR (~ 2011 bp) and FR (~ 1408 bp), consistent with in silico predictions. Following transient transfection of HEK293T cells, expression of the target proteins was evaluated at 48 h post-transfection. SDS–PAGE and Western blot analysis revealed specific bands at approximately 70 kDa (PEDV-S-RBD-FR) and 40 kDa (FR), confirming successful expression of the recombinant proteins in mammalian cells (Fig. 1B-D).

Figure 1. Construction and expression of recombinant PEDV-S-RBD-ferritin expression plasmids. (A) Schematic diagram of the recombinant expression constructs. The receptor-binding domain (RBD) of the PEDV spike (S) protein was genetically fused to the N-terminus of Helicobacter pylori ferritin (FR) via a flexible linker. A Kozak sequence, GT6 signal peptide, and 10×His tag were introduced upstream of the S-RBD sequence to facilitate efficient expression and purification. The recombinant genes were cloned into the pCAGGS vector using EcoR I and Hind III restriction sites to generate pCAGGS-PEDV-S-RBD-FR and pCAGGS-FR. (B) Restriction enzyme analysis of the recombinant plasmids. Plasmids were digested with EcoR I and Hind III, yielding the expected fragments corresponding to the pCAGGS backbone (4244 bp) and the insert fragments of PEDV-S-RBD-FR (~ 2011 bp) or FR (~ 1408 bp), confirming successful plasmid construction. (C) SDS–PAGE analysis of recombinant protein expression in HEK293T cells. Cell lysates were collected 48 h after transient transfection with pCAGGS-PEDV-S-RBD-FR or pCAGGS-FR and analyzed by SDS–PAGE. Protein bands corresponding to PEDV-S-RBD-FR (~ 70 kDa) and FR (~ 40 kDa) were detected, indicating successful expression of the recombinant proteins. (D) Western blot analysis of recombinant protein expression. Proteins expressed in HEK293T cells were analyzed by Western blot using an anti-His monoclonal antibody. Specific immunoreactive bands corresponding to PEDV-S-RBD-FR (~ 70 kDa) and FR (~ 40 kDa) confirmed expression of the recombinant proteins.

Production and validation of recombinant lentiviruses

Correct construction of the lentiviral shuttle plasmids was verified by EcoR I and BamH I digestion, which produced fragments consistent with the expected sizes, including the 8172 bp pLVX-IRES-ZsGreen1 backbone and the corresponding insert fragments (Fig. 2A). Recombinant lentiviruses were generated by co-transfecting HEK293T cells with the transfer vector, psPAX2, and pMD2.G plasmids at a ratio of 3:2:1. At 48 h post-transfection, strong GFP fluorescence was observed, indicating efficient transfection and successful lentiviral packaging (Fig. 2B). Viral supernatants were subsequently harvested for downstream experiments.

Expression and purification of ferritin-based fusion proteins

ExpiCHO cells were transduced with recombinant lentiviruses at an MOI of 20. GFP fluorescence was detected at 48 h post-transduction, confirming efficient gene delivery (Fig. 3A). Expression of the PEDV-S-RBD-FR and FR proteins was first confirmed in crude cell lysates by SDS–PAGE (Fig. 3B). Following large-scale culture, recombinant proteins were purified by His-tag affinity chromatography. Distinct bands corresponding to approximately 72 kDa (PEDV-S-RBD-FR) and 40 kDa (FR) were observed in the purified fractions, consistent with the predicted molecular weights (Fig. 3C). Western blot analysis further confirmed the specificity of the purified proteins (Fig. 3D).

Self-assembly and morphological characterization of nanoparticles

Transmission electron microscopy (TEM) was used to assess nanoparticle formation. Both PEDV-S-RBD-FR and FR proteins exhibited spherical nanoparticle structures with relatively uniform size distribution (Fig. 3E, F). Particle size analysis showed that PEDV-S-RBD-FR nanoparticles had an average diameter of 27.37 nm, whereas FR nanoparticles exhibited an average diameter of 15.10 nm (Fig. 3E, F). These results indicate that fusion of the PEDV S-RBD antigen increased nanoparticle size while preserving the self-assembly properties of the ferritin scaffold.

Humoral immune responses induced by immunization

The immunization schedule is shown in Fig. 4A. Serum samples collected on days 0, 14, 28, and 42 post-immunization were analyzed for antigen-specific IgG responses. No specific antibodies were detected prior to immunization. By day 14, both the PEDV-S-RBD-FR and FR groups exhibited detectable antigen-specific IgG responses. After booster immunization, IgG titers in the PEDV-S-RBD-FR group increased to 1:40,960, significantly higher than in the PBS control group (Fig. 4B). These results demonstrate that the ferritin-based nanoparticles effectively induces a strong antigen-specific humoral immune response.

Induction of PEDV-specific neutralizing antibodies

The functional activity of immune sera was evaluated by virus neutralization test (VNT) combined with indirect immunofluorescence assay (IFA). Serum samples collected at day 42 post-immunization were tested for neutralizing activity against PEDV. The PEDV-S-RBD-FR group exhibited a neutralizing antibody titer of 1:64 (Fig. 4C). Infected Vero cells in this group showed intact morphology with no detectable cytopathic effect (CPE), whereas severe CPE was observed in the PBS control group. Consistent with the VNT results, IFA analysis showed an absence of fluorescence signal in the PEDV-S-RBD-FR group, indicating complete inhibition of viral infection, whereas strong fluorescence was observed in control samples. These findings demonstrate that the ferritin-based nanoparticle vaccine induces not only binding antibodies but also functional neutralizing antibodies capable of blocking PEDV infection in vitro.

Cytokine responses induced by vaccination

Serum levels of IFN-γ and IL-4 were quantified by ELISA at different time points post-immunization (Fig. 4D, E). Both cytokines were significantly elevated in the PEDV-S-RBD-FR group compared with the PBS control group throughout the study period. As representative Th1- and Th2-type cytokines, IFN-γ and IL-4 reflect cellular and humoral immune activation, respectively. Notably, the IFN-γ/IL-4 ratio remained above 1 at day 42, indicating a Th1-biased mixed immune response induced by the vaccine formulation.

Discussion

The present study demonstrates that a ferritin-based nanoparticle can serve as an effective platform for multivalent presentation of the PEDV S-RBD antigen, resulting in enhanced humoral and cellular immune responses. By combining mammalian expression with ferritin self-assembly, the recombinant nanoparticle preserved structural integrity while eliciting functional neutralizing antibodies, highlighting the feasibility of ferritin as a vaccine platform against PEDV [19, 20].

Ferritin has emerged as an attractive vaccine scaffold because its highly ordered 24-mer architecture enables repetitive antigen display, a structural feature known to promote efficient B-cell receptor cross-linking and antigen uptake by antigen-presenting cells [21, 22]. Consistent with these characteristics, fusion of the PEDV S-RBD to ferritin preserved nanoparticle assembly while increasing particle size, suggesting successful surface presentation of the antigen without compromising structural integrity. Such multivalent organization is expected to improve antigen stability and immune recognition, thereby contributing to the enhanced immunogenicity observed in the present work [21]. Recent studies have further demonstrated that ferritin-based nanoparticle vaccines can elicit broad-spectrum protective immune responses against coronaviruses and other viral pathogens, supporting the translational potential of this platform [14]. Notably, a phase 1 clinical trial of a SARS-CoV-2 spike ferritin nanoparticle vaccine adjuvanted with Army Liposome Formulation reported favorable safety and immunogenicity profiles in humans, underscoring the clinical viability of this approach.

Beyond inducing antigen-specific antibodies, the ferritin nanoparticle vaccine generated functional neutralizing activity capable of preventing PEDV infection in vitro. The preservation of conformational epitopes on the RBD, together with the repetitive antigen arrangement on the nanoparticle surface, likely contributed to this neutralizing capacity [19]. Although the neutralizing antibody titer remained moderate, the ability to block viral infection supports the biological relevance of the immune response and demonstrates the potential of ferritin-mediated antigen display to improve vaccine efficacy [19, 23]. The cytokine profile further suggested coordinated activation of both humoral and cellular immunity, with a gradual predominance of Th1-associated responses at later stages. Such a balanced immune profile is considered advantageous for antiviral vaccines, as it promotes both antibody-mediated neutralization and cellular mechanisms involved in viral clearance.

Despite these encouraging findings, several important issues remain to be addressed before this vaccine platform can be translated into practical application. First, the immunogenicity of the ferritin-based PEDV vaccine candidate was evaluated only in a mouse model, and its protective efficacy in the natural host remains to be demonstrated; future studies should therefore assess vaccine-induced protection in piglet challenge models to validate its translational potential. Second, because PEDV is an enteric pathogen, mucosal immune responses, particularly intestinal immunity, are essential for effective protection but were not examined in the present study. Recent advances in mucosal vaccine delivery, including oral recombinant Lactobacillus vectors expressing PEDV S antigens and intranasal adenovirus vaccines encoding PEDV COE, have shown promising results in inducing intestinal IgA and lactogenic immunity [24, 25]. Exploring mucosal vaccination strategies, such as intranasal or oral immunization [26], and characterizing both systemic and mucosal immune responses will therefore be important. Third, although the vaccine elicited functional neutralizing antibodies with a titer of 1:64, the magnitude of the humoral response remained moderate, suggesting that further optimization of antigen density, spatial arrangement on the ferritin scaffold, and adjuvant formulation may improve immunogenicity. In addition, the durability of vaccine-induced immunity was not investigated and should be evaluated in long-term follow-up studies. From a translational perspective, future work should also establish scalable manufacturing processes using CHO cell-based bioreactor systems and evaluate cross-protective

efficacy against emerging PEDV variants to determine the breadth and practical applicability of this vaccine platform.

Conclusion

A ferritin-based nanoparticle displaying the PEDV S-RBD elicited robust antigen-specific humoral and cellular immune responses and generated functional neutralizing antibodies in mice. These findings support ferritin as a promising platform for PEDV vaccine development, integrating structural stability, multivalent antigen presentation, and enhanced immune activation. Although additional studies in piglets, together with evaluation of mucosal immunity and long-term protection, are required, the present work provides a foundation for the development of next-generation nanoparticle vaccines against PEDV.

Declarations

Ethics approval and consent to participate

All animal experiments were conducted in accordance with the national Regulations on the Administration of Experimental Animals from China's Ministry of Science and Technology. The experimental protocol was approved by the Scientific Ethics Committee of Jiangsu Agri-animal Husbandry Vocational College (Permit No. JSAHVC-2025-108).

Consent for publication

Not applicable.

Competing interests

The authors declare no competing interests.

Funding

This work was supported by the Qinglan Project of Jiangsu Province and the the project of Jiangsu Agri-animal Husbandry Vocational College, grant number NSF2026ZR04.

Author Contribution

MZ, SC, and SZ conceived and designed the study. NN, MZ, LZ, and SC performed the experiments and analyzed the data. MZ, SC, and CC developed and executed the experimental design, including laboratory methodology and analytical validation. MZ prepared the initial draft of the manuscript. All authors reviewed and edited the manuscript, and read and approved the final version.

Acknowledgements

The authors would like to thank the support of Jiangsu Key Laboratory for High-Tech Research and Development of Veterinary Biopharmaceuticals. This research was funded by the Qinglan Project of Jiangsu Province, the Agricultural Support Project of Taizhou (TN202415), and the project of Jiangsu Agri-animal Husbandry Vocational College (grant number NSF2026ZR04).

Data Availability

All data supporting the findings of this study are included in the published article and its supplementary files. The raw experimental data and statistical analysis files are available from the corresponding author upon reasonable request.

References

1. Xu H, Wu H, Min J, et al. Effective control of the emerging PEDV G2-c variant with an inactivated autogenous vaccine. Front Vet Sci. 2025;12:1697499. https://doi.org/10.3389/fvets.2025.1697499.
2. Yang Q, Zhang Y, Chen L, Fang L, Xiao S. Isolation, pathogenicity, and an infectious cDNA clone of the prevalent G2c variant of porcine epidemic diarrhea virus in China. Microb Pathog. 2025;205:107637. https://doi.org/10.1016/j.micpath.2025.107637.
3. Zhuang L, Zhao Y, Shen J, et al. Advances in porcine epidemic diarrhea virus research: genome, epidemiology, vaccines, and detection methods. Discov Nano. 2025;20(1):48. https://doi.org/10.1186/s11671-025-04220-y.
4. Li YY, Fan CH, Li HX, et al. Emergence of a Highly Virulent Porcine Epidemic Diarrhea Virus (PEDV) G2c Subtype in China: Isolation, Genetic and Pathogenic Characterization, and Cross-Neutralizing Antibody Response. Transbound Emerg Dis. 2026;2026:3811264. https://doi.org/10.1155/tbed/3811264.
5. Zhao Y, Fan B, Song X, et al. PEDV-spike-protein-expressing mRNA vaccine protects piglets against PEDV challenge. mBio. 2024;15(2):e0295823. https://doi.org/10.1128/mbio.02958-23.
6. Li W, Hangalapura BN, van den Elzen P, et al. Safety and efficacy of live attenuated PEDV vaccines for neonatal protection. NPJ Vaccines. 2025;10(1):131. https://doi.org/10.1038/s41541-025-01195-w.
7. Hsieh CL, Goldsmith JA, Schaub JM, et al. Structure-based design of prefusion-stabilized SARS-CoV-2 spikes. Science. 2020;369(6510):1501–5. https://doi.org/10.1126/science.abd0826.
8. Guo W, Wang C, Song X, et al. Immunogenicity and protective efficacy of a trimeric full-length S protein subunit vaccine for porcine epidemic diarrhea virus. Vaccine. 2024;42(4):828–39. https://doi.org/10.1016/j.vaccine.2024.01.020.
9. Li L, Yin S, Zhou J, et al. Spike 1 trimer, a nanoparticle vaccine against porcine epidemic diarrhea virus induces protective immunity challenge in piglets. Front Microbiol. 2024;15:1386136.

https://doi.org/10.3389/fmicb.2024.1386136.

10. Ma X, Zou F, Yu F, et al. Nanoparticle Vaccines Based on the Receptor Binding Domain (RBD) and Heptad Repeat (HR) of SARS-CoV-2 Elicit Robust Protective Immune Responses. Immunity. 2020;53(6):1315–e309. https://doi.org/10.1016/j.immuni.2020.11.015.
11. Wang W, Huang B, Zhu Y, Tan W, Zhu M. Ferritin nanoparticle-based SARS-CoV-2 RBD vaccine induces a persistent antibody response and long-term memory in mice. Cell Mol Immunol. 2021;18(3):749–51. https://doi.org/10.1038/s41423-021-00643-6.
12. Masuda A, Lee JM, Miyata T, et al. Stable trimer formation of spike protein from porcine epidemic diarrhea virus improves the efficiency of secretory production in silkworms and induces neutralizing antibodies in mice. Vet Res. 2021;52(1):102. https://doi.org/10.1186/s13567-021-00971-5.
13. Hu G, Luo X, Liao J, et al. Neutralizing antibody levels as a key factor in determining the immunogenic efficacy of the novel PEDV alpha coronavirus vaccine. Vet Q. 2025;45(1):1–20. https://doi.org/10.1080/01652176.2025.2509506.
14. Wang W, Meng X, Cui H, et al. Self-assembled ferritin-based nanoparticles elicit a robust broad-spectrum protective immune response against SARS-CoV-2 variants. Int J Biol Macromol. 2024;264(Pt 2):130820. https://doi.org/10.1016/j.ijbiomac.2024.130820.
15. Hills RA, Tan TK, Cohen AA, et al. Proactive vaccination using multiviral Quartet Nanocages to elicit broad anti-coronavirus responses. Nat Nanotechnol. 2024;19(8):1216–23. https://doi.org/10.1038/s41565-024-01655-9.
16. Joyce MG, Chen WH, Sankhala RS, et al. SARS-CoV-2 ferritin nanoparticle vaccines elicit broad SARS coronavirus immunogenicity. Cell Rep. 2021;37(12):110143. https://doi.org/10.1016/j.celrep.2021.110143.
17. Chang X, Ma J, Zhou Y, Xiao S, Xiao X, Fang L. Development of a Ferritin Protein Nanoparticle Vaccine with PRRSV GP5 Protein. Viruses. 2024;16(6). https://doi.org/10.3390/v16060991.
18. Tang P, Cui E, Cheng J, et al. A ferritin nanoparticle vaccine based on the hemagglutinin extracellular domain of swine influenza A (H1N1) virus elicits protective immune responses in mice and pigs. Front Immunol. 2024;15:1361323. https://doi.org/10.3389/fimmu.2024.1361323.
19. Liu Y, Deng J, Bi Z, Luo M, Han X, Yao L. Ferritin-based nanoparticle vaccine protects neonatal piglets against porcine epidemic diarrhea virus challenge following immunization of pregnant sows. Vet Res. 2025;56(1):140. https://doi.org/10.1186/s13567-025-01542-8.
20. Gu J, Zheng X, Li C, et al. A bacteriophage-based virus-like particle vaccine induces cross-reactive neutralising antibodies against porcine epidemic diarrhoea viruses (PEDV). Vet Res. 2025;56(1):128. https://doi.org/10.1186/s13567-025-01559-z.
21. Cao S, Ma D, Ji S, Zhou M, Zhu S. Self-Assembled Ferritin Nanoparticles for Delivery of Antigens and Development of Vaccines: From Structure and Property to Applications. Molecules. 2024;29(17). https://doi.org/10.3390/molecules29174221.
22. Ahmadivand S, Gomez-Casado E. Advances in Nanoparticles as Vaccine Adjuvants. Vaccines (Basel). 2026;14(2):159. https://doi.org/10.3390/vaccines14020159.

23. Walls AC, Fiala B, Schäfer A, et al. Elicitation of Potent Neutralizing Antibody Responses by Designed Protein Nanoparticle Vaccines for SARS-CoV-2. Cell. 2020;183(5):1367–e8217. https://doi.org/10.1016/j.cell.2020.10.043.
24. Yan S, Luo Y, Zhan N, et al. Intranasal delivery of a recombinant adenovirus vaccine encoding the PEDV COE elicits potent mucosal and systemic antibody responses in mice. Microbiol Spectr. 2024;12(10):e0069224. https://doi.org/10.1128/spectrum.00692-24.
25. Zhang B, Gou H, Shen H, et al. Display of porcine epidemic diarrhea virus spike protein B-cell linear epitope on Lactobacillus mucosae G01 S-layer surface induce a robust immunogenicity in mice. Microb Cell Fact. 2024;23(1):142. https://doi.org/10.1186/s12934-024-02409-x.
26. Li Q, Xu Z, Wu T, et al. A flagellin-adjuvanted PED subunit vaccine improved protective efficiency against PEDV variant challenge in pigs. Vaccine. 2018;36(29):4228–35. https://doi.org/10.1016/j.vaccine.2018.05.124.

Figures

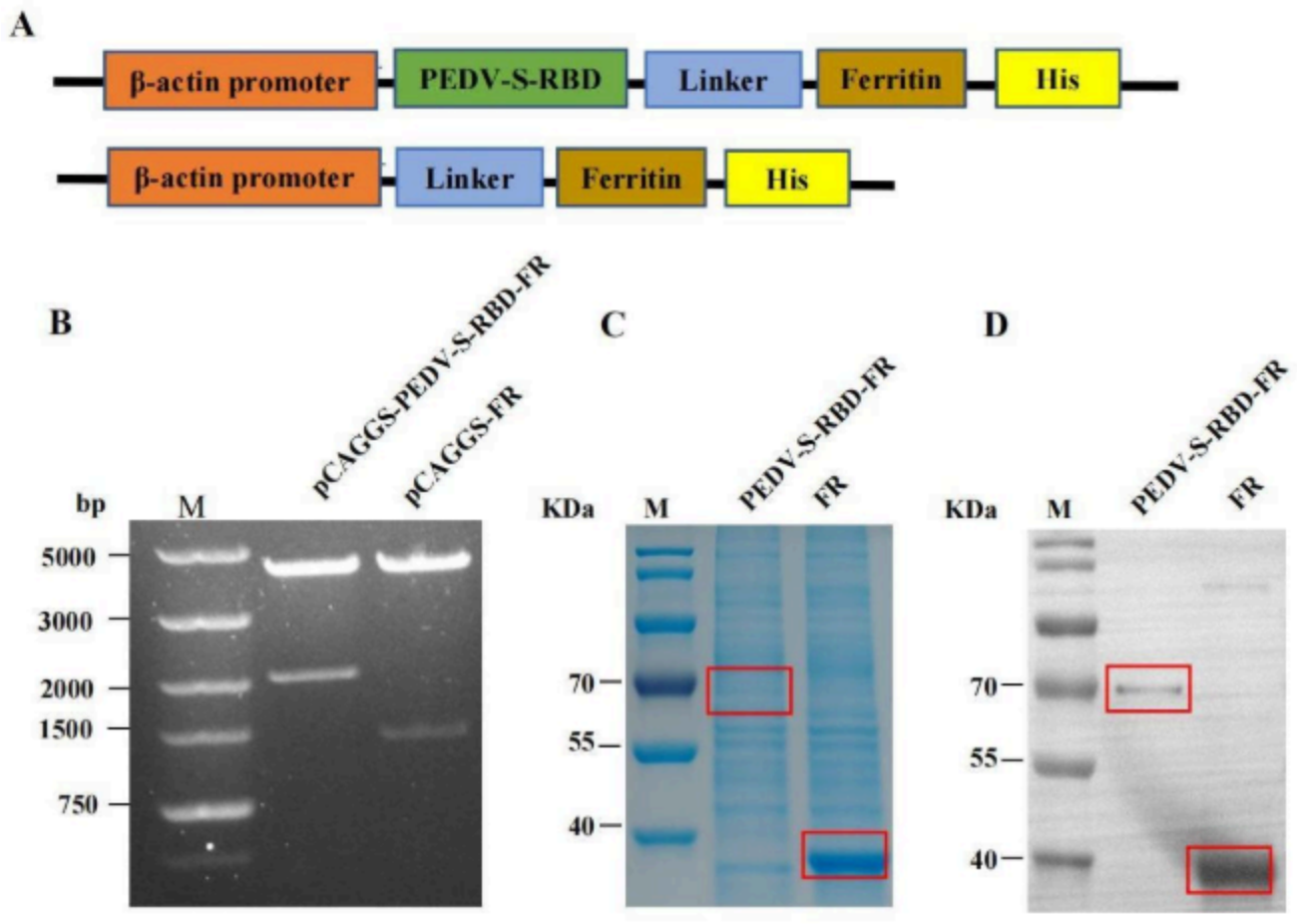


Figure 1

Construction and expression of recombinant PEDV-S-RBD-ferritin expression plasmids. (A) Schematic diagram of the recombinant expression constructs. The receptor-binding domain (RBD) of the PEDV

spike (S) protein was genetically fused to the N-terminus of Helicobacter pylori ferritin (FR) via a flexible linker. A Kozak sequence, GT6 signal peptide, and 10×His tag were introduced upstream of the S-RBD sequence to facilitate efficient expression and purification. The recombinant genes were cloned into the pCAGGS vector using EcoR I and Hind III restriction sites to generate pCAGGS-PEDV-S-RBD-FR and pCAGGS-FR. (B) Restriction enzyme analysis of the recombinant plasmids. Plasmids were digested with EcoR I and Hind III, yielding the expected fragments corresponding to the pCAGGS backbone (4244 bp) and the insert fragments of PEDV-S-RBD-FR (~2011 bp) or FR (~1408 bp), confirming successful plasmid construction. (C) SDS–PAGE analysis of recombinant protein expression in HEK293T cells. Cell lysates were collected 48 h after transient transfection with pCAGGS-PEDV-S-RBD-FR or pCAGGS-FR and analyzed by SDS–PAGE. Protein bands corresponding to PEDV-S-RBD-FR (~70 kDa) and FR (~40 kDa) were detected, indicating successful expression of the recombinant proteins. (D) Western blot analysis of recombinant protein expression. Proteins expressed in HEK293T cells were analyzed by Western blot using an anti-His monoclonal antibody. Specific immunoreactive bands corresponding to PEDV-S-RBD-FR (~70 kDa) and FR (~40 kDa) confirmed expression of the recombinant proteins.

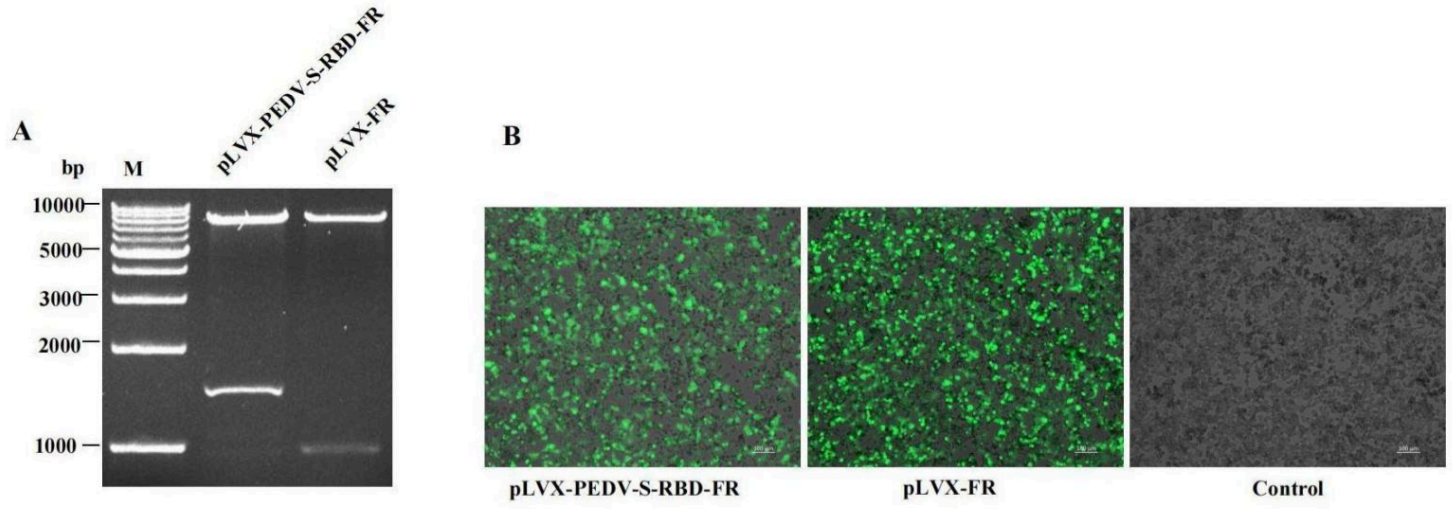


Figure 2

Construction and validation of recombinant lentiviruses. (A) Restriction digestion analysis of recombinant lentiviral plasmids. The pLVX-PEDV-S-RBD-FR and pLVX-FR plasmids were digested with EcoR I and BamH I. The pLVX-PEDV-S-RBD-FR plasmid showed an ~8172 bp pLVX-IRES-ZsGreen1 backbone and an insert fragment, whereas pLVX-FR showed only the backbone fragment, confirming correct plasmid construction. M, DNA marker (bp). (B) GFP fluorescence detection in HEK293T cells at 48 h post-transfection. Strong green fluorescence was observed in both pLVX-PEDV-S-RBD-FR- and pLVX-FR-transfected cells, indicating efficient transfection and successful lentiviral packaging. No fluorescence was detected in the non-transfected control group.

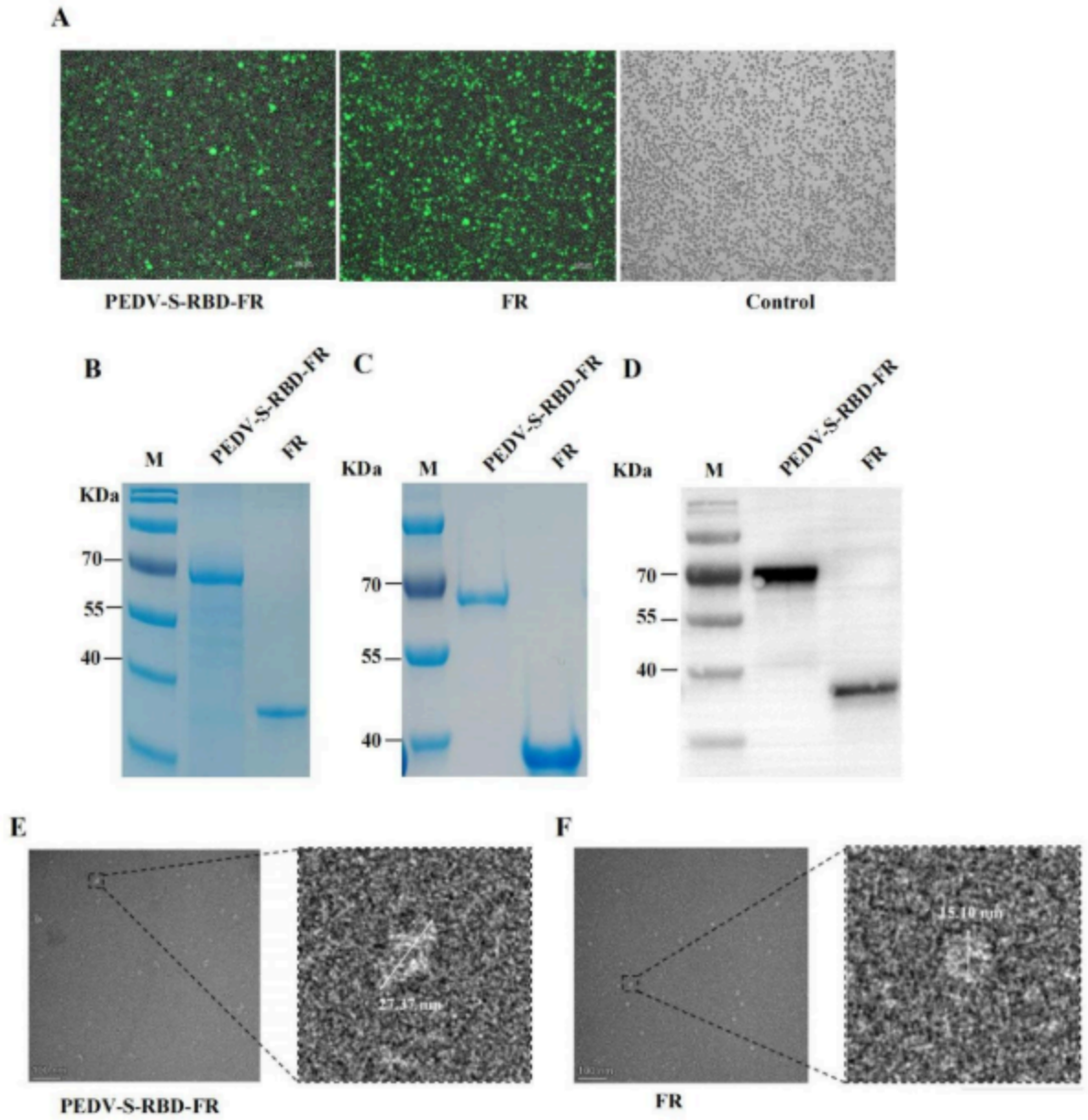


Figure 3

Expression, purification, and morphological characterization of ferritin-based fusion proteins. (A) GFP fluorescence detection in ExpiCHO cells at 48 h post-transduction. Strong green fluorescence was observed in PEDV-S-RBD-FR- and FR-transduced cells, confirming efficient gene delivery. No fluorescence was detected in the non-transduced control group. (B) SDS–PAGE analysis of crude cell lysates. Red boxes indicate the target protein bands of PEDV-S-RBD-FR (~72 kDa) and FR (~40 kDa). M, protein marker (kDa). (C) SDS–PAGE analysis of purified proteins after His-tag affinity chromatography. Distinct bands corresponding to PEDV-S-RBD-FR (~72 kDa) and FR (~40 kDa) were observed. (D) Western blot analysis confirming the specificity of purified PEDV-S-RBD-FR and FR proteins. (E) TEM images of PEDV-S-RBD-FR nanoparticles. Left panel, overall morphology; right panel, magnified view with particle size measurement (average diameter, 27.37 nm). (F) TEM images of FR nanoparticles. Left panel, overall morphology; right panel, magnified view with particle size measurement (average diameter, 15.10 nm).

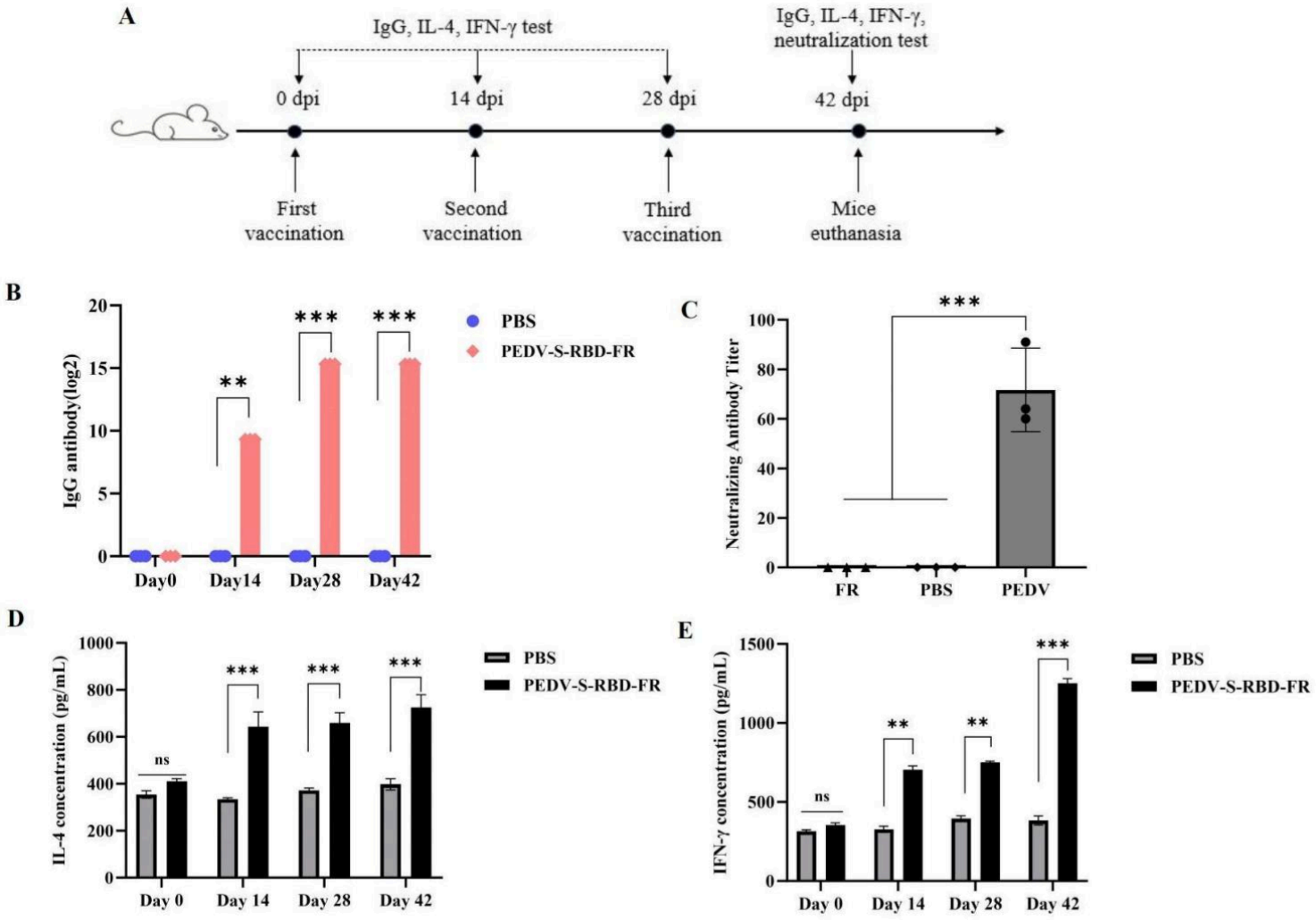


Figure 4

Humoral immune responses, neutralizing antibody production, and cytokine profiles induced by PEDV-S-RBD-FR nanoparticle vaccination in mice. (A) Schematic illustration of the immunization and sampling schedule. Mice were immunized three times, on days 0, 14, and 28, and serum samples were collected on days 0, 14, 28, and 42 post-immunization (dpi) for IgG, IL-4, and IFN-γ detection. At day 42, mice were euthanized for additional IgG, IL-4, IFN-γ, and neutralization assays. (B) Kinetics of antigen-specific IgG antibody responses in immunized mice. Serum IgG titers (log2) were measured by ELISA on days 0, 14, 28, and 42 post-immunization. The PEDV-S-RBD-FR group showed significantly higher IgG titers than the PBS control group at all time points after primary immunization (mean ± SD; ****P < 0.0001). (C) PEDV-specific neutralizing antibody titers at day 42 post-immunization. The PEDV-S-RBD-FR group exhibited a neutralizing antibody titer of 1:64, significantly higher than the FR and PBS control groups (***P < 0.001). (D) Serum IL-4 concentrations at different time points post-immunization. IL-4 levels were significantly elevated in the PEDV-S-RBD-FR group compared with the PBS control group at days 14, 28, and 42 dpi, with no significant difference at day 0 (***P < 0.001; ****P < 0.0001). (E) Serum IFN-γ concentrations at different time points post-immunization. IFN-γ levels were significantly elevated in the PEDV-S-RBD-FR

group compared with the PBS control group at days 14, 28, and 42 dpi, with no significant difference at day 0.